Composite Structures 92 (2010) 1888–1895

Contents lists available at ScienceDirect

Composite Structures

journal homepage: www.elsevier.com/locate/compstruct

MITC technique extended to variable kinematic multilayered plate elements

E. Carrera [a], M. Cinefra [a,b,*], P. Nali [a]

[a] Department of Aeronautics and Space Engineering, Politecnico di Torino, Torino, Italy
[b] CRP H. Tudor, Esch-sur-Alzette, Luxembourg

ARTICLE INFO

Article history:
Available online 1 February 2010

Keywords:
MITC
Carrera Unified Formulation
Refined theories
Shear locking
Multilayered structures

ABSTRACT

This paper considers the Mixed Interpolation of Tensorial Components (MITC) technique, which was originally proposed for Reissner–Mindlin type plates to develop shear locking free refined multilayered plate elements. Refined elements are obtained by referring to variable kinematic modelling in the framework of the Carrera Unified Formulation (CUF): linear, parabolic, cubic and fourth-order displacement fields in the thickness direction of the plate are used; both equivalent single layer (the multilayered plate is considered as an equivalent one-layer plate) and layer-wise (each layer is considered as an independent plate) variable descriptions are accounted for. Four-node elements are considered and a number of applications are developed for isotropic and multilayered anisotropic plates. Results related to the mixed interpolation of tensorial components are compared to the reduced and selective integration technique in the static and dynamic linear analysis. The numerical results show that the MITC technique maintains its effectiveness in the case of variable kinematic plate elements, hence the obtained elements are free from shear locking mechanisms. The capability of MITC to reduce/remove spurious modes is confirmed for refined multilayered elements.

1. Introduction

The shear locking phenomena in Reissner–Mindlin type finite elements (FEs) remains a milestone in finite elements analysis. Shear locking consists of a numerical difficulty (in the convergence rate sense) of reducing Reissner–Mindlin plate/shell elements to exact or Kirchhoff–Love solutions in the case of thin plate/shell analysis. The inclusion of both bending and shear stiffness in a unique rotational degree of freedom, in fact, makes it difficult to obtain zero-transverse-shear-energy in thin shell structures, as in physics. The mesh convergence rate becomes very small and a huge number of elements would be necessary to fulfill the zero-transverse-shear-energy constraint. A pioneering remedy, proposed in the late 1960's- early 1970's, is based on a reduced and/or selective numerical integration technique of transverse shear stiffness contributions. The reduced integration permits a significant increase of the convergence rate through the evaluation of the transverse shear strain energy in a plate integration point in which the corresponding shear strains are very small. The problem has been clearly explained and dealt with in detail in many FE books, such as those by Zienkiewic [1], Bathe [2] and Hughes [3], among others.

Unfortunately reduced integration techniques, since they introduce, 'by definition', an additional error into the evaluation of stiffness matrices, could lead to an increase in spurious and/or hourglass type 'non-physical' deformation modes which could destroy the related FE solutions. Such a drawback cannot be accepted especially in the case of nonlinear analysis, in which previous load-step solutions (which can be largely affected by spurious modes) are used to build the current equilibrium (e.g., with the Newton–Raphson method application). Non-convergent solution can be obtained in practical applications.

A remedy to this problem was introduced by many authors in the 80's. In particular, reference can be made to the work by Bathe and Dvorkin [4], even though similar works (earlier and/or later) by Mc Neal [5], Huang and Hinton [6] and Jang et al. [7] are known. In [4], the remedy was stated as Mixed Interpolation of Tensorial Components (MITC) and was first proposed for linear four node Q4 plate/shell elements. Subsequent work led to the extension to eight node Q8 elements. The MITC formulation permits the transverse shear locking phenomenon to be eliminated by introducing an independent FE approximation into the element domains for the transverse shear strains. Other authors have preferred to call this remedy as 'assumed shear strain field concept', as in [8]. A more rigorous mathematical justification of the MITC technique was established in the framework of the so-called Babuska–Brezzi

* Corresponding author. Address: Department of Aeronautics and Space Engineering, Politecnico di Torino, Corso Duca degli Abruzzi 24, 10129 Torino, Italy. Tel.: +39 011 090 6869; fax: +39 011 090 6899.
E-mail addresses: erasmo.carrera@polito.it (E. Carrera), maria.cinefra@polito.it (M. Cinefra), pietro.nali@polito.it (P. Nali).

0263-8223/$ - see front matter © 2010 Elsevier Ltd. All rights reserved.
doi:10.1016/j.compstruct.2010.01.009

conditions [9]. Further studies on the MITC method for Reissner–Mindlin problems were provided by Brezzi et al. [10] and Della Croce et al. [11,12].

Over the last decade, the first author has proposed the Carrera Unified Formulation (CUF) [13–16], for the analysis of layered structures. CUF permits a large variety of plate/shell theories as well as FEs, with variable kinematic and hierarchical properties, to be handled in a unified manner, on the basis of few so-called 'fundamental nuclei'. Refined Equivalent Single Layer (ESL) and Layer-Wise (LW) models have been used; the number of independent variables is maintained independent by the number of the constitutive layers N_l in the ESL models, while the unknown variables are independent in each layer in the LW models. The shear locking mechanism, in the related FE method, has been contrasted by using reduced/selective integration techniques, which lead to satisfactory results in the case of geometrically linear problems [17]. Extension to FE analysis of smart structures has been also provided in [18,19]. The present work aims at extending the MITC technique to variable kinematic models for the case of plate elements with four nodes. The aim is twofold: 1. to prove that the extension of MITC to higher-order (ESL and LW models) plate elements is feasible and 2. to show that such an extension is numerically efficient. The paper is organized as follows: Section 2 briefly recalls the original MITC technique for the case of Reissner–Mindlin plate theories; Section 3 shows the variable kinematic modelling in the CUF framework; Section 4 formulates the extension of the MITC technique to CUF by deriving the corresponding fundamental nuclei; Section 5 shows the obtained numerical results. The conclusions are drawn in the last section.

2. The MITC technique

A four node plate bending element, based on the Mindlin–Reissner plate theory and mixed interpolation, was proposed by Bathe and Dvorkin in [4]. The Mixed Interpolation Tensorial Component (MITC4) method calculates the transverse shear stresses σ_{xz} and σ_{yz} in a different manner from other tensorial components. Shear stresses are approximated in sample points of the domain Ω (see Fig. 1).

According to the Mindlin–Reissner theory, the displacement field is modelled as follows:

$$\begin{aligned} u_i &= u_i^0 + z\phi_i \quad i = x, y \\ u_z &= u_z^0 \end{aligned} \tag{1}$$

where ϕ_x, ϕ_y are the rotations of the normals to the reference surfaces x–z and y–z, respectively; the apex^0 denotes a quantity calculated on Ω. By introducing the FE approximation, the displacement field is described by the relation:

$$\{u_x^0, u_y^0, u_z, \phi_x, \phi_y\} = \{N\}^T\{q\} \tag{2}$$

where $\{N\}$ denotes the vector of the interpolating Lagrange shape functions and $\{q\}$ is the vector of the nodal degrees of freedom. The dimension of $\{q\}$ is $5 \cdot nn$, where nn is the number of finite element nodes, in this case $nn = 4$.

Hooke's law can be conveniently written for a generic layer by splitting the bending (b) and shear (s) contributions:

$$\begin{Bmatrix} \{\sigma_b\} \\ \{\sigma_s\} \end{Bmatrix} = \begin{bmatrix} [Q_b] & [0] \\ [0] & [Q_s] \end{bmatrix} \begin{Bmatrix} \{\varepsilon_b\} \\ \{\varepsilon_s\} \end{Bmatrix} \tag{3}$$

The geometrical relations permit the strains ε_b and ε_s to be written as a function of the displacements, therefore:

$$\varepsilon_b = \begin{Bmatrix} u_{x,x}^0 \\ u_{y,y}^0 \\ u_{x,y}^0 + u_{y,x}^0 \end{Bmatrix} + z \begin{Bmatrix} \phi_{x,x} \\ \phi_{y,y} \\ \phi_{x,y} + \phi_{y,x} \end{Bmatrix}, \quad \varepsilon_s = \begin{Bmatrix} \phi_x + u_{z,x} \\ \phi_y + u_{z,y} \end{Bmatrix} \tag{4}$$

In matrix form:

$$\{\varepsilon_b\} = [B_b]q, \quad \{\varepsilon_s\} = [B_s]q \tag{5}$$

According to MITC4, the transverse shear strains are interpolated assuming the following shear strain field (see Fig. 1):

$$\{\varepsilon_s\} = \begin{Bmatrix} \{\varepsilon_{xz}\} \\ \{\varepsilon_{yz}\} \end{Bmatrix} = \begin{Bmatrix} \frac{1}{2}(1+\xi)\varepsilon_{xz}^N + \frac{1}{2}(1-\xi)\varepsilon_{xz}^Q \\ \frac{1}{2}(1+\eta)\varepsilon_{yz}^P + \frac{1}{2}(1-\eta)\varepsilon_{yz}^M \end{Bmatrix} \tag{6}$$

where M, N, P and Q are sample points and ξ, η are the natural coordinates in the plane of the element. The relations between the global coordinates x, y and the natural coordinates ξ, η are the following:

$$\begin{aligned} x &= \sum_{j=1}^{N_n} x_j N_j(\xi, \eta) \\ y &= \sum_{j=1}^{N_n} y_j N_j(\xi, \eta) \end{aligned} \tag{7}$$

with $-1 < \xi, \eta < 1$. N_j is the Lagrange shape function relative to node j.

In this way, the stiffness matrix K is written in two contributions (bending and shear):

$$\begin{aligned} &[K] = [K_b] + [K_s] \\ &[K_b] = \langle [B_b]^T [Q_b][B_b] \rangle; \quad [K_s] = \langle [B_s]^T [Q_s][B_s] \rangle \end{aligned} \tag{8}$$

where the following notation has been introduced:

$$\langle \ldots \rangle = \sum_{k=1}^{ns} \int_{V_k} (\ldots) dV_k \tag{9}$$

where ns is the number of layers and V_k is the volume of the layer k.

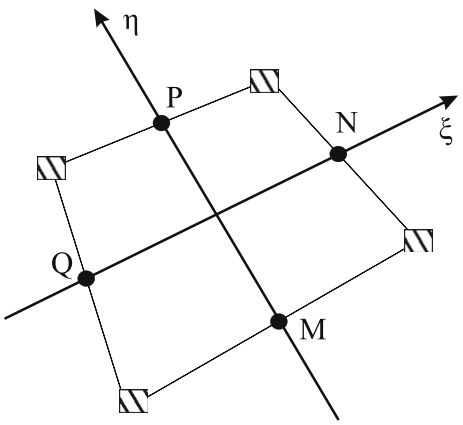

Fig. 1. Sample points (M, N, P, Q) to approximate the shear contribution in the MITC4 element.

3. Variable kinematic model via Carrera Unified Formulation

Carrera Unified Formulation (CUF) is a technique which handles a large variety of bi-dimensional models in a unified manner. According to CUF, the governing equations are written in terms of a few fundamental nuclei which do not formally depend on the order of expansion N used in the z direction and on the description of variables: ESL or LW. The application of a two-dimensional method for plates permits to express the unknown variables as a set of thickness functions depending only on the thickness coordinate z and the corresponding variables depending on the in plane coordinates x and y. So that, a generic variable, for instance the

displacement $u(x,y,z)$, and its variation $\delta u(x,y,z)$ are written according to the following general expansion:

$$\begin{aligned}\boldsymbol{u}(x,y,z) &= F_\tau(z)\boldsymbol{u}_\tau(x,y), \quad \delta\boldsymbol{u}(x,y,z)\\ &= F_\tau(z)\delta\boldsymbol{u}_\tau(x,y), \quad \text{with} \quad \tau,s=0,\ldots,N\end{aligned} \tag{10}$$

Bold letters denote arrays and the summing convention with repeated indexes τ and s is assumed. The order of expansion N goes from first to higher-order values and, depending on the used thickness functions, a model can be ESL or LW. If the variable is assumed for the whole multilayer, the approach is ESL and a Taylor expansion is employed as thickness function $F(z)$:

$$\boldsymbol{u} = F_0\boldsymbol{u}_0 + F_1\boldsymbol{u}_1 + \ldots + F_N\boldsymbol{u}_N = F_\tau\boldsymbol{u}_\tau \text{ with } \tau = 0,1,\ldots,N \tag{11}$$

$$F_0 = z^0 = 1,\ F_1 = z^1 = z,\ \ldots,\ F_N = z^N \tag{12}$$

When the description is LW the variable is considered independent in each layer:

$$\boldsymbol{u^k} = F_t\boldsymbol{u}_t^k + F_b\boldsymbol{u}_b^k + F_l\boldsymbol{u}_l^k \quad \text{with} \quad l=2,\ldots,N \tag{13}$$

where t and b indicate the top and bottom of the plate and the thickness functions $F(z)$ are combinations of Legendre polynomials:

$$\begin{aligned}&P_0 = 1, \quad P_1 = \zeta_k, \quad P_2 = \frac{(3\zeta_k^2-1)}{2}, \quad P_3 = \frac{5\zeta_k^3}{2} - \frac{3\zeta_k}{2},\\ &P_4 = \frac{35\zeta_k^4}{8} - \frac{15\zeta_k^2}{4} + \frac{3}{8}\end{aligned} \tag{14}$$

$$\begin{aligned}&F_t = \frac{P_0+P_1}{2}, \quad F_b = \frac{P_0-P_1}{2}, \quad F_l = P_l - P_{l-2} \quad \text{with}\\ &l=2,\ldots,N\end{aligned} \tag{15}$$

The chosen functions have the following interesting properties:

$$\begin{aligned}&\zeta_k = 1 : F_t = 1; \quad F_b = 0; \quad F_l = 0 \text{ at top}\\ &\zeta_k = -1 : F_t = 0; \quad F_b = 1; \quad F_l = 0 \text{ at bottom}\end{aligned} \tag{16}$$

that is the interface values of the variables are considered as unknowns.

It is possible to obtain the FSDT model [20,21] from an ESL theory with first order of expansion, by considering a constant transverse displacement through the thickness. An appropriate application of penalty techniques to shear correction factor leads to CLT [22].

4. Extension of MITC to CUF

This section presents the derivation of the governing finite element stiffness matrix based on the *Principle of Virtual Displacements* (PVD) in case of a multilayered plate subjected to mechanical loads. CUF permits to obtain the so-called *fundamental nuclei* which are simple matrices representing the basic elements from which the stiffness matrix of the whole structure can be computed. The MITC technique of the previous paragraph, is herein extended to CUF.

The PVD for a plate with N_l layers, under mechanical loads, reads:

$$\sum_{k=1}^{N_l}\int_{\Omega_k}\int_{A_k}\left\{\delta\boldsymbol{\varepsilon}_{pG}^{k\ T}\boldsymbol{\sigma}_{pC}^k + \delta\boldsymbol{\varepsilon}_{nG}^{k\ T}\boldsymbol{\sigma}_{nC}^k\right\}d\Omega_k\,dz = \sum_{k=1}^{N_l}\delta L_e^k \tag{17}$$

where Ω_k and A_k are the integration domains in plane (x,y) and z direction, respectively. k indicates the layer and T the transpose of a vector. The first member of the equation represents the variation of internal work δL_{int}^k, while δL_e^k is the external work for the kth layer. G means geometrical relations and C constitutive ones.

The first step to derive the FE matrices is the substitution of *constitutive equations* (C) in the variational statement PVD:

$$\begin{aligned}\boldsymbol{\sigma}_{pC}^k &= \boldsymbol{C}_{pp}^k\boldsymbol{\varepsilon}_{pG}^k + \boldsymbol{C}_{pn}^k\boldsymbol{\varepsilon}_{nG}^k\\ \boldsymbol{\sigma}_{nC}^k &= \boldsymbol{C}_{np}^k\boldsymbol{\varepsilon}_{pG}^k + \boldsymbol{C}_{nn}^k\boldsymbol{\varepsilon}_{nG}^k\end{aligned} \tag{18}$$

with

$$\begin{aligned}\boldsymbol{C}_{pp}^k &= \begin{bmatrix} C_{11} & C_{12} & C_{16}\\ C_{12} & C_{22} & C_{26}\\ C_{16} & C_{26} & C_{66}\end{bmatrix} \quad \boldsymbol{C}_{pn}^k = \begin{bmatrix} 0 & 0 & C_{13}\\ 0 & 0 & C_{23}\\ 0 & 0 & C_{36}\end{bmatrix}\\ \boldsymbol{C}_{np}^k &= \begin{bmatrix} 0 & 0 & 0\\ 0 & 0 & 0\\ C_{13} & C_{23} & C_{36}\end{bmatrix} \quad \boldsymbol{C}_{nn}^k = \begin{bmatrix} C_{55} & C_{45} & 0\\ C_{45} & C_{44} & 0\\ 0 & 0 & C_{33}\end{bmatrix}\end{aligned} \tag{19}$$

The second step consists to introduce *geometrical relations*, which relate the strains to the displacement components $\boldsymbol{u} = (u_x, u_y, u_z)$:

$$\begin{aligned}\boldsymbol{\varepsilon}_{pG}^k &= \boldsymbol{D}_p^k\ \boldsymbol{u}^k,\\ \boldsymbol{\varepsilon}_{nG}^k &= (\boldsymbol{D}_{n\Omega}^k + \boldsymbol{D}_{nz}^k)\ \boldsymbol{u}^k\end{aligned} \tag{20}$$

wherein the differential operator arrays are defined as follows:

$$\boldsymbol{D}_p^k = \begin{bmatrix}\partial_x & 0 & 0\\ 0 & \partial_y & 0\\ \partial_y & \partial_x & 0\end{bmatrix}, \quad \boldsymbol{D}_{n\Omega}^k = \begin{bmatrix}0 & 0 & \partial_x\\ 0 & 0 & \partial_y\\ 0 & 0 & 0\end{bmatrix}, \quad \boldsymbol{D}_{nz}^k = \begin{bmatrix}\partial_z & 0 & 0\\ 0 & \partial_z & 0\\ 0 & 0 & \partial_z\end{bmatrix} \tag{21}$$

By introducing the unified formulation for the displacements (Eq. (10)), one has:

$$\begin{aligned}\boldsymbol{\varepsilon}_{pG}^k &= \boldsymbol{D}_p^k\ (F_\tau\boldsymbol{u}_\tau^k),\\ \boldsymbol{\varepsilon}_{nG}^k &= (\boldsymbol{D}_{n\Omega}^k + \boldsymbol{D}_{nz}^k)(F_\tau\boldsymbol{u}_\tau^k) = \boldsymbol{D}_{n\Omega}^k(F_\tau\boldsymbol{u}_\tau^k) + F_{\tau_z}\boldsymbol{u}_\tau^k\end{aligned} \tag{22}$$

Finally, it is possible to express the displacement $\boldsymbol{u}_\tau^k$ as a function of *nodal displacements* $\boldsymbol{q}_{\tau i}^k$, by means of *shape functions*:

$$\boldsymbol{u}_\tau^k = N_i\boldsymbol{q}_{\tau i}^k \quad (i=1,2,\ldots,N_n) \tag{23}$$

with $\boldsymbol{q}_{\tau i}^k = (q_{u_x\tau i}^k,\ q_{u_y\tau i}^k,\ q_{u_z\tau i}^k)$. N_n is the number of nodes of the element and N_i is the shape function relative to node i. Therefore, the geometrical relations become:

$$\begin{aligned}\boldsymbol{\varepsilon}_{pG}^k &= F_\tau\boldsymbol{D}_p^k\ (N_i\boldsymbol{I})\boldsymbol{q}_{\tau i}^k,\\ \boldsymbol{\varepsilon}_{nG}^k &= F_\tau\boldsymbol{D}_{n\Omega}^k(N_i\boldsymbol{I})\boldsymbol{q}_{\tau i}^k + F_{\tau_z}N_i\boldsymbol{q}_{\tau i}^k\end{aligned} \tag{24}$$

According to MITC, the transverse strain array $\boldsymbol{\varepsilon}_n$ can be written as:

$$\{\boldsymbol{\varepsilon}_n\} = \begin{Bmatrix}\boldsymbol{\varepsilon}_{13}\\ \boldsymbol{\varepsilon}_{23}\\ \boldsymbol{\varepsilon}_{33}\end{Bmatrix} = \begin{Bmatrix}\frac{1}{2}(1+\xi)\boldsymbol{\varepsilon}_{13}^N + \frac{1}{2}(1-\xi)\boldsymbol{\varepsilon}_{13}^Q\\ \frac{1}{2}(1+\eta)\boldsymbol{\varepsilon}_{23}^P + \frac{1}{2}(1-\eta)\boldsymbol{\varepsilon}_{23}^M\\ \boldsymbol{\varepsilon}_{33}\end{Bmatrix} \tag{25}$$

In matrix form:

$$\{\boldsymbol{\varepsilon}_n\} = \begin{bmatrix}\frac{1}{2}(1+\xi) & \frac{1}{2}(1-\xi) & 0 & 0 & 0\\ 0 & 0 & \frac{1}{2}(1+\eta) & \frac{1}{2}(1-\eta) & 0\\ 0 & 0 & 0 & 0 & 1\end{bmatrix}\begin{Bmatrix}\boldsymbol{\varepsilon}_{13}^N\\ \boldsymbol{\varepsilon}_{13}^Q\\ \boldsymbol{\varepsilon}_{23}^P\\ \boldsymbol{\varepsilon}_{23}^M\\ \boldsymbol{\varepsilon}_{33}\end{Bmatrix} \tag{26}$$

The relations (24) permit to express the transverse shear strain in the sample points (N,Q,P,M) as a function of nodal displacements:

$$\begin{Bmatrix} \varepsilon^N_{13} \\ \varepsilon^Q_{13} \\ \varepsilon^P_{23} \\ \varepsilon^M_{23} \\ \varepsilon_{33} \end{Bmatrix} = \begin{bmatrix} 0 & 0 & F_\tau N_{i,x}(N) \\ 0 & 0 & F_\tau N_{i,x}(Q) \\ 0 & 0 & F_\tau N_{i,y}(P) \\ 0 & 0 & F_\tau N_{i,y}(M) \\ 0 & 0 & 0 \end{bmatrix} \boldsymbol{q}_{\tau i} + \begin{bmatrix} F_{\tau_z} N_i(N) & 0 & 0 \\ F_{\tau_z} N_i(Q) & 0 & 0 \\ 0 & F_{\tau_z} N_i(P) & 0 \\ 0 & F_{\tau_z} N_i(M) & 0 \\ 0 & 0 & F_{\tau_z} N_i \end{bmatrix} \boldsymbol{q}_{\tau i} \tag{27}$$

Introducing the following notation:

$$N_a = \frac{1}{2}(1+\xi),\ N_b = \frac{1}{2}(1-\xi),\ N_c = \frac{1}{2}(1+\eta),\ N_d = \frac{1}{2}(1-\eta) \tag{28}$$

the relation between the transverse strain and the nodal displacements can be rewritten as:

$$\boldsymbol{\varepsilon}^k_{n_\tau i} = F_\tau[\boldsymbol{C}_{1i}]\boldsymbol{q}^k_{\tau i} + F_{\tau_z}[\boldsymbol{C}_{2i}]\boldsymbol{q}^k_{\tau i} \tag{29}$$

where

$$[\boldsymbol{C}_{1i}] = \begin{bmatrix} 0 & 0 & N_a N_{iN,x} + N_b N_{iQ,x} \\ 0 & 0 & N_c N_{iP,y} + N_d N_{iM,y} \\ 0 & 0 & 0 \end{bmatrix}$$
$$[\boldsymbol{C}_{2i}] = \begin{bmatrix} N_a N_{iN} + N_b N_{iQ} & 0 & 0 \\ 0 & N_c N_{iP} + N_d N_{iM} & 0 \\ 0 & 0 & N_i \end{bmatrix} \tag{30}$$

Similarly, the transverse stress has the following expression:

$$\boldsymbol{\sigma}^k_{n_\tau i} = [\boldsymbol{C}_{nn}]^k \left(F_\tau[\boldsymbol{C}_{1i}]\boldsymbol{q}^k_{\tau i} + F_{\tau_z}[\boldsymbol{C}_{2i}]\boldsymbol{q}^k_{\tau i}\right) \tag{31}$$

Substituting $\boldsymbol{\sigma}_p$, $\boldsymbol{\sigma}_n$, $\boldsymbol{\varepsilon}_p$ and $\boldsymbol{\varepsilon}_n$ in the PVD, the governing equation is obtained:

$$\delta L^k_{int} = \delta \boldsymbol{q}^{kT}_{\tau i} \boldsymbol{K}^{k\tau sij} \boldsymbol{q}^k_{sj} \tag{32}$$

The explicit form of fundamental nucleo $\boldsymbol{K}^{k\tau sij}$ is given in the Appendix A.

5. Numerical analysis and discussion

A numerical investigation has been implemented to assess the effectiveness of the assumed shear strain field concept for the case of plate elements based on higher-order displacement models as well as on a layer-wise variable description.

The corresponding analytical solutions (*A*), obtained using the closed form solution proposed in [13,14], are used for comparison purposes. The assumed shear strain field solutions (MITC4) are compared with various numerical integration schemes: Normal (*N*) (2×2 Gauss points), Reduced (*R*) (1×1 Gauss point) and Selective (*S*) 1×1 Gauss points for bending stiffness and 1×1 for transverse shear stiffness contributions).

Isotropic as well as layered plates are considered. The material data are given in Tables 1 and 2, respectively, and the geometry of the cross ply laminated plate is reported in Fig. 2. The results are restricted to non-dimensional transverse displacement $\bar{w} = \frac{w \cdot 100 E_T h^3}{p_z^+ a^4}$, calculated in the center of the simply supported plate and up to forth-order of expansion in the thickness direction for both ESL and LW models. The plate is subjected to bisinusoidal load in the *z* direction:

$$p_z^+ = \hat{p}_z^+ \sin\left(\frac{m\pi x}{a}\right) \sin\left(\frac{n\pi y}{b}\right) \tag{33}$$

where *m* and *n* are the wave numbers and $\hat{p}_z^+ = 10^3$ Pa is the amplitude of the load. The considered theories are indicated in the tables with the acronyms ESL-N and LW-N, that are ESL and LW theories, respectively, based on the PVD variational statement, with order of expansion *N* in the thickness direction. A 15×15 mesh and a square plate geometry, with plate dimensions $a = b = 1$ m, have been adopted.

The FSDT results are first considered in Table 3 for the case of isotropic material made plates. Various integration schemes are compared to the analytical solution and MITC technique. The shear locking mechanism is clearly evident for the thin plate case and Normal integration cases. The MITC4 element prevents shear locking without any sub-integration scheme; as is known, and will be

Table 1
Material data: Aluminium plate.

Aluminio	
E)	72.0 GPa
G	27.1 GPa
v	0.33
ρ	2810 Kg/m^2

Table 2
Material data: graphite/epoxy orthotropic plate (0°/90°/0°).

Gr/Ep	
E_1	132.38 GPa
E_2	10.756 GPa
E_3	10.756 GPa
$G_1 2$	3.606 GPa
$G_1 3$	5.6537 GPa
$G_2 3$	5.6537 GPa
$v_1 2$	0.24
$v_1 3$	0.24
$v_2 3$	0.49

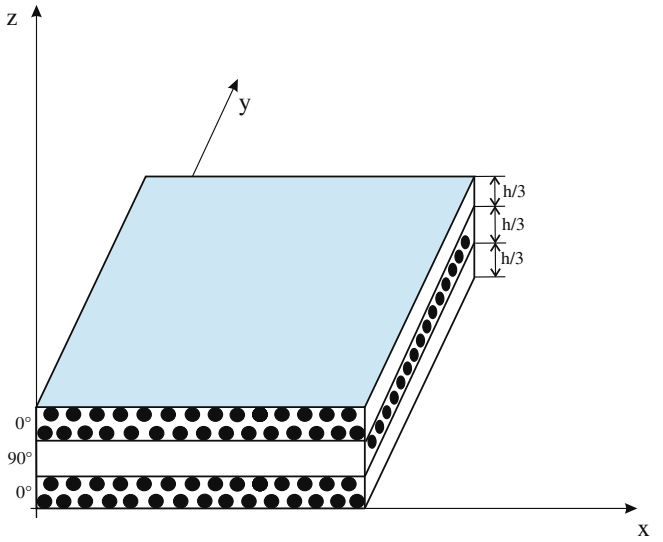

Fig. 2. Geometry of graphite/epoxy orthotropic plate.

Table 3
Transversal displacement $\bar{w}$ at the center of the isotropic plate. Theory FSDT.

$w_c(z=0)$	$a/h = 10$	$a/h = 50$	$a/h = 100$	$a/h = 500$	$a/h = 1000$
A	2.8780	2.7487	2.7446	2.7434	2.7432
N	2.6718	0.9571	0.3236	0.0146	0.0037
R	2.8683	2.7386	2.7346	2.7333	2.7331
S	2.8616	2.7320	2.7279	2.7266	2.7266
MITC	2.8611	2.7316	2.7279	2.7266	2.7266

briefly discussed later on, this happens because of the great reduction in the possible spurious modes.

Higher-order theory results, related to a parabolic distribution of the displacements field, are given in Table 4. It appears clear from that table that the MITC method also works in the case of FEs formulated on the basis of higher-order theories, that is, the *shear locking phenomenon does not depend on the order of the displacement field in the plate thickness*. Table 5 confirms this for the case of the third order displacement field. Higher-order theories obviously lead to more deformable structures in the case of thick plates; this fact, however, does not depend on shear locking: it is instead due to the higher transverse shear deformability of thick plates. Layer-wise results are given in Tables 6 and 7. These theories only have displacement variables as degrees of freedom. With respect to shear locking, layer-wise theories behave exactly like the FSDT and ESL cases, that is, the MITC method remains effective in both equivalent single layer and layer-wise variable description cases.

A cross-ply laminated plate is considered in Tables 8–12. It is possible to conclude, for all the considered theories, that shear locking and the MITC behave exactly as in the isotropic one-layer plate case.

A compendium of the made analysis, in the case of very thin plates is given in Tables 13 and 14 for metallic and composite plates, respectively. The capacity of the MITC technique to remain efficient in the CUF framework of the modelling of layered plates is evident.

Table 4
Transversal displacement $\bar{w}$ at the center of the isotropic plate. Theory ESL-2.

$w_c(z=0)$	$a/h=10$	$a/h=50$	$a/h=100$	$a/h=500$	$a/h=1000$
A	2.8657	2.7482	2.7445	2.7434	2.7432
N	2.6591	0.9567	0.3236	0.0146	0.0037
R	2.8561	2.7382	2.7345	2.7333	2.7331
S	2.8479	2.7299	2.7262	2.7250	2.7252
MITC	2.8474	2.7298	2.7261	2.7250	2.7252

Table 5
Transversal displacement $\bar{w}$ at the center of the isotropic plate. Theory ESL-3.

$w_c(z=0)$	$a/h=10$	$a/h=50$	$a/h=100$	$a/h=500$	$a/h=1000$
A	2.8845	2.7490	2.7447	2.7434	2.7432
N	2.6754	0.9568	0.3236	0.0146	0.0037
R	2.8749	2.7389	2.7346	2.7333	2.7331
S	2.8667	2.7306	2.7263	2.7250	2.7252
MITC	2.8661	2.7306	2.7263	2.7250	2.7252

Table 6
Transversal displacement $\bar{w}$ at the center of the isotropic plate. Theory LW-2.

$w_c(z=0)$	$a/h=10$	$a/h=50$	$a/h=100$	$a/h=500$	$a/h=1000$
A	2.8657	2.7482	2.7445	2.7434	2.7432
N	2.6592	0.9567	0.3236	0.0146	0.0037
R	2.8561	2.7382	2.7345	2.7333	2.7331
S	2.8479	2.7299	2.7262	2.7250	2.7252
MITC	2.8474	2.7298	2.7361	2.7250	2.7252

Table 7
Transversal displacement $\bar{w}$ at the center of the isotropic plate. Theory LW-4.

$w_c(z=0)$	$a/h=10$	$a/h=50$	$a/h=100$	$a/h=500$	$a/h=1000$
A	2.8844	2.7490	2.7447	2.7434	2.7432
N	2.6754	0.9568	0.3236	0.0146	0.0037
R	2.8749	2.7389	2.7346	2.7333	2.7338
S	2.8667	2.7306	2.7263	2.7250	2.7245
MITC	2.8661	2.7306	2.7263	2.7249	2.7245

Table 8
Transversal displacement $\bar{w}$ at the center of the multilayered plate. Theory FSDT.

$w_c(z=0)$	$a/h=10$	$a/h=50$	$a/h=100$	$a/h=500$	$a/h=1000$
A	0.9278	0.7767	0.7720	0.7705	0.7704
N	0.9020	0.4868	0.2294	0.0128	0.0032
R	0.9245	0.7732	0.7684	0.7668	0.7668
S	0.9220	0.7706	0.7658	0.7643	0.7642
MITC	0.9215	0.7706	0.7658	0.7643	0.7642

Table 9
Transversal displacement $\bar{w}$ at the center of the multilayered plate. Theory ESL-2.

$w_c(z=0)$	$a/h=10$	$a/h=50$	$a/h=100$	$a/h=500$	$a/h=1000$
A	0.9249	0.7767	0.7720	0.7705	0.7704
N	0.9001	0.4871	0.2294	0.0128	0.0032
R	0.9227	0.7739	0.7692	0.7677	0.7676
S	0.9200	0.7713	0.7666	0.7650	0.7650
MITC	0.9195	0.7713	0.7666	0.7650	0.7650

Table 10
Transversal displacement $\bar{w}$ at the center of the multilayered plate. Theory ESL-3.

$w_c(z=0)$	$a/h=10$	$a/h=50$	$a/h=100$	$a/h=500$	$a/h=1000$
A	0.9730	0.7788	0.7725	0.7705	0.7704
N	0.9457	0.4879	0.2295	0.0129	0.0032
R	0.9709	0.7760	0.7697	0.7677	0.7676
S	0.9683	0.7733	0.7671	0.7651	0.7650
MITC	0.9676	0.7733	0.7671	0.7651	0.7650

Table 11
Transversal displacement $\bar{w}$ at the center of the multilayered plate. Theory LW-2.

$w_c(z=0)$	$a/h=10$	$a/h=50$	$a/h=100$	$a/h=500$	$a/h=1000$
A	0.9805	0.7791	0.7726	0.7705	0.7704
N	0.9527	0.4880	0.2295	0.0128	0.0032
R	0.9784	0.7763	0.7698	0.7677	0.7676
S	0.9758	0.7737	0.7672	0.7651	0.7650
MITC	0.9750	0.7737	0.7672	0.7651	0.7650

Table 12
Transversal displacement $\bar{w}$ at the center of the multilayered plate. Theory LW-4.

$w_c(z=0)$	$a/h=10$	$a/h=50$	$a/h=100$	$a/h=500$	$a/h=1000$
A	0.9809	0.7791	0.7726	0.7705	0.7704
N	0.9531	0.4880	0.2295	0.0128	0.0032
R	0.9788	0.7763	0.7698	0.7677	0.7672
S	0.9762	0.7737	0.7672	0.7650	0.7633
MITC	0.9754	0.7737	0.7672	0.7650	0.7632

Table 13
Transversal displacement $\bar{w}$ at the center of the isotropic plate. Thickness ratio $a/h=1000$.

$w_c(z=0)$	*A*	*N*	*R*	*S*	MITC
FSDT	2.7432	0.0037	2.7331	2.7266	2.7266
$ESL-1$	2.7432	0.0037	2.7331	2.7266	2.7266
$ESL-2$	2.7432	0.0037	2.7331	2.7252	2.7252
$ESL-3$	2.7432	0.0037	2.7331	2.7252	2.7252
$ESL-4$	2.7432	0.0037	2.7331	2.7252	2.7252
$LW-1$	2.7432	0.0037	2.0700	2.0657	2.0657
$LW-2$	2.7432	0.0037	2.7331	2.7252	2.7252
$LW-3$	2.7432	0.0037	2.7331	2.7252	2.7252
$LW-4$	2.7432	0.0037	2.7338	2.7245	2.7245

Spurious modes are briefly discussed in Table 15. It is known that these 'unphysical modes' are problem dependent (on the material, geometries, mesh, loadings, etc). Table 15 compares the Selective integration scheme with MITC results. Previous analysis, related to the evaluation of plate center deflection, have shown small differences between S and MITC results. The differences become more evident when the higher vibration response is checked. For the sake of simplicity, attention has here been restricted to LW-1 analysis and beam-type geometries. The considered beam is made of Aluminium, with dimensions $a = 1$ m, $b = 0.1$ m and thickness $h = 0.1$ m; it is simply supported along the y direction and free along x. Q4 plate elements are used for the analysis and the adopted meshes are 30×1, 200×1 and 300×2. The first 40 frequencies are given in Hz. Spurious modes are highlighted by an asterisk. These have been checked and, for the sake of brevity, have not been shown in this work.

Table 15 confirms that shear locking phenomenon reduces by mesh increasing: spurious vibration modes move to higher-order frequencies in both S and MITC cases. However, MITC FE element, compared to Selective integration cases, shows two main advantages: it greatly reduces spurious modes; it moves the spurious modes (if any) to higher-order frequencies. To be noticed the difficulties of FE plate model to detect beam vibration modes transverse to the reference surface Ω; the beam has a square section and refined mesh must be used to find double modes. However, that point does not affect the discussion on spurious modes.

Table 14
Transversal displacement $\bar{w}$ at the center of the multilayered plate. Thickness ratio $a/h = 1000$.

$w_c(z=0)$	A	N	R	S	MITC
FSDT	0.7704	0.0032	0.7668	0.7642	0.7642
$ESL-1$	0.7704	0.0032	0.7668	0.7642	0.7642
$ESL-2$	0.7704	0.0032	0.7676	0.7650	0.7650
$ESL-3$	0.7704	0.0032	0.7676	0.7650	0.7650
$ESL-4$	0.7704	0.0032	0.7676	0.7650	0.7650
$LW-1$	0.7652	0.0032	0.7624	0.7598	0.7598
$LW-2$	0.7704	0.0032	0.7676	0.7650	0.7650
$LW-3$	0.7704	0.0032	0.7678	0.7649	0.7647
$LW-4$	0.7704	0.0032	0.7672	0.7633	0.7632

6. Concluding remarks

In this paper, the MITC method has been extended to refined models (in the framework of the Unified Formulation by Carrera) to prevent the shear locking phenomenon in finite plate elements. Isotropic as well as multilayered plates have been considered and they have been analyzed using different theories in both the static and dynamic case. The MITC technique results have been compared with other numerical integration schemes results, such as

Table 15
Natural frequencies in (Hz) of an Aluminium beam. Theory LW-1.

n	Mesh (30×1)		Mesh (200×1)		Mesh (300×2)	
	(S)	(MITC)	(S)	(MITC)	(S)	(MITC)
2	24.3483*	24.3483	20.3704*	24.3122	24.2939	24.2939
3	38.6542*	53.2660	24.3122	26.0570	24.3117	24.3117
4	53.2657	97.7909	26.0570*	97.2120	97.1329	97.1330
5	97.7909*	213.5543	81.4421*	104.1822	97.2037	97.2045
6	154.9560*	221.5323	97.2120	218.5894	218.3887	218.3895
7	213.5497	397.6177	104.1812*	234.2383	218.5473	218.5512
8	221.5323*	482.3379	183.0969*	388.2620	387.8490	387.8516
9	349.9235*	628.9913	218.5894	415.9980	388.1291	388.1415
10	397.6178	862.0786	234.2334*	605.9767	605.2194	605.2257
11	482.3148*	919.5792	325.1388*	649.1461	605.6532	605.6833
12	625.2562*	1274.4017	388.2620	871.4115	870.1253	870.1383
13	628.9913	1356.2359*	415.9827*	933.2822	870.7433	870.8055
14	862.0057	1553.4594*	507.2958*	1184.1786	1182.1159	1182.1399
15	919.5793*	1699.7146	605.9767	1267.9249	1182.9464*	1183.0607
16	983.3359*	1969.27456	649.1088*	1543.8272*	1437.5753*	1540.7081
17	1274.4017	2203.1852	729.2222*	1552.7658*	1540.6676	1541.9296*
18	1356.0586*	2532.6474	871.4115	1652.5152	1541.7360	1552.7569*
19	1427.2268*	2706.6672	933.2053*	1949.8471	1945.1880	1945.2525
20	1699.7146*	2794.1037*	990.5014*	2086.4225	1946.5168	1946.8243
21	1960.6679*	3111.1787*	1184.1786	2401.6727	2395.0213	2395.1189
22	1968.9087	3483.6325	1267.7831*	2530.9717	2396.6294	2397.0938
23	2203.1852	3574.8850	1290.6488*	2568.9487	2530.9470*	2530.9470
24	2532.6474*	4285.0908	1543.8272*	2898.6871	2875.2005*	2889.5946
25	2588.0549*	4581.3664*	1629.1165*	3099.3350*	2889.4529	2892.0283*
26	2705.9940	4677.4287*	1652.2750	3105.6274*	2891.3552*	3105.5564*
27	2794.1037*	5075.5161	1949.8471*	3440.2267	3105.3929*	3427.9134
28	3314.4023*	5214.2676	2005.2968*	3676.7673	3427.7146	3430.8646
29	3483.6326	5734.4497*	2086.0404	4025.5857	3429.9218	4009.2618
30	3573.7473*	6256.5008*	2328.9033	4300.3824	4008.9906	4012.7916
31	4145.2761*	6289.7471	2401.6727*	4654.0210*	4011.5084*	4632.7837
32	4285.0908	7043.2504	2418.5268*	4658.6805*	4312.9253*	4636.9559*
33	4579.5665	7533.2118	2530.9716	4969.2746	4632.4228	4658.4410*
34	5075.5161*	7638.9288	2568.3711*	5062.0898	4635.2518	5061.8929
35	5086.6807*	7852.7127	2868.0935*	5324.7568	5061.8929	5297.5866
36	5214.2676	8517.4587	2898.6871	5682.5015	5297.1163	5302.4671
37	5731.7504*	8969.6656	3098.4969*	6036.9894*	5300.2514*	6002.7471
38	6144.8816*	9470.4077	3353.2385*	6212.0210*	5750.7997*	6008.4033*
39	6289.7471	10167.0191	3440.2267	6439.0906	6002.1455	6211.4534*
40	7039.3813	10233.4095	3675.5916	6789.8919	6005.5756	6747.3161

Spurious modes are highlighted by an asterisk.

Normal, Reduced and Selective integration. From this analysis it is possible to conclude that:

- The MITC method is as effective as Selective integration in contrasting the shear locking phenomenon in the static case.
- The MITC method remains effective in the case of FEs formulated on the basis of higher-order theories and in both ESL and LW variable description cases.
- In the case of cross-ply laminated plates, MITC behaves exactly in the same way as for isotropic one-layer plates.
- The dynamic analysis shows that MITC, compared with Selective integration, reduces spurious modes and moves them to higher frequencies, especially by refining the mesh.

Future work could be directed towards shell formulation as well as geometrically nonlinear problems.

Acknowledgments

Authors acknowledge the partial support of Piemonte Regional Project STEPS. M Cinefra acknowledges the support of FNR of Luxembourg.

Appendix A

The explicit expression of the fundamental nucleo $\boldsymbol{K}^{k\tau sij}$ is proposed below.

Introducing the following notation:

$$\lhd \ldots \rhd_\Omega = \int_\Omega \ldots d\Omega \tag{34}$$

the fundamental nucleo $K^{k\tau sij}$ can be written as:

$$\begin{aligned}
K_{xx}^{k\tau sij} &= C_{55}^k N_{iN} N_{jN} \lhd N_a N_a \rhd_\Omega F_{s,z} F_{\tau,z} + C_{55}^k N_{iN} N_{jQ} \lhd N_b N_a \rhd_\Omega F_{s,z} F_{\tau,z} \\
&+ C_{55} N_{iN}^k N_{jQ} \lhd N_a N_b \rhd_\Omega F_{s,z} F_{\tau,z} + C_{55} N_{iQ}^k N_{jQ} \lhd N_b N_b \rhd_\Omega F_{s,z} F_{\tau,z} \\
&+ C_{11}^k \lhd N_{i,x} N_{j,x} \rhd_\Omega F_s F_\tau + C_{16}^k \lhd N_{i,y} N_{j,x} \rhd_\Omega F_s F_\tau + C_{16}^k \\
&\lhd N_{i,x} N_{j,y} \rhd_\Omega F_s F_\tau + C_{66}^k \lhd N_{i,y} N_{j,y} \rhd_\Omega F_s F_\tau
\end{aligned}$$

$$\begin{aligned}
K_{yx}^{k\tau sij} &= C_{45}^k N_{iM} N_{jN} \lhd N_d N_a \rhd_\Omega F_{s,z} F_{\tau,z} + C_{45}^k N_{iM} N_{jN} \lhd N_c N_a \rhd_\Omega F_{s,z} F_{\tau,z} \\
&+ C_{45}^k N_{iM} N_{jQ} \lhd N_d N_b \rhd_\Omega F_{s,z} F_{\tau,z} + C_{45}^k N_{iP} N_{jQ} \lhd N_c N_b \rhd_\Omega F_{s,z} F_{\tau,z} \\
&+ C_{16}^k \lhd N_{i,x} N_{j,x} \rhd_\Omega F_s F_\tau + C_{12}^k \lhd N_{i,y} N_{j,x} \rhd_\Omega F_s F_\tau + C_{66}^k \\
&\lhd N_{i,x} N_{j,y} \rhd_\Omega F_s F_\tau + C_{26}^k \lhd N_{i,y} N_{j,y} \rhd_\Omega F_s F_\tau
\end{aligned}$$

$$\begin{aligned}
K_{zx}^{k\tau sij} &= C_{45}^k N_{i,yM} N_{jN} \lhd N_d N_a \rhd_\Omega F_{s,z} F_\tau + C_{45}^k N_{i,yM} N_{jQ} \\
&\lhd N_d N_b \rhd_\Omega F_{s,z} F_\tau + C_{55}^k N_{i,xN} N_{jN} \lhd N_a N_a \rhd_\Omega F_{s,z} F_\tau \\
&+ C_{55}^k N_{i,xN} N_{jQ} \lhd N_a N_b \rhd_\Omega F_{s,z} F_\tau + C_{45}^k N_{i,yP} N_{jN} \\
&\lhd N_c N_a \rhd_\Omega F_{s,z} F_\tau + C_{45}^k N_{i,yP} N_{jQ} \lhd N_c N_b \rhd_\Omega F_{s,z} F_\tau \\
&+ C_{55}^k N_{i,xQ} N_{jN} \lhd N_b N_a \rhd_\Omega F_{s,z} F_\tau + C_{55}^k N_{i,xQ} N_{jQ} \\
&\lhd N_b N_b \rhd_\Omega F_{s,z} F_\tau + C_{13}^k \lhd N_i N_{j,x} \rhd_\Omega F_s F_{\tau,z} + C_{36}^k \\
&\lhd N_i N_{j,y} \rhd_\Omega F_s F_{\tau,z}
\end{aligned} \tag{35}$$

$$\begin{aligned}
K_{xy}^{k\tau sij} &= C_{45}^k N_{iN} N_{jM} \lhd N_a N_d \rhd_\Omega F_{s,z} F_{\tau,z} + C_{45}^k N_{iQ} N_{jM} \lhd N_b N_d \rhd_\Omega F_{s,z} F_{\tau,z} \\
&+ C_{45}^k N_{iN} N_{jP} \lhd N_a N_c \rhd_\Omega F_{s,z} F_{\tau,z} + C_{45}^k N_{iQ} N_{jP} \lhd N_b N_c \rhd_\Omega F_{s,z} F_{\tau,z} \\
&+ C_{16}^k \lhd N_{i,x} N_{j,x} \rhd_\Omega F_s F_\tau + C_{66}^k \lhd N_{i,y} N_{j,x} \rhd_\Omega F_s F_\tau + C_{12}^k \\
&\lhd N_{i,x} N_{j,y} \rhd_\Omega F_s F_\tau + C_{26}^k \lhd N_{i,y} N_{j,y} \rhd_\Omega F_s F_\tau
\end{aligned}$$

$$\begin{aligned}
K_{yy}^{k\tau sij} &= C_{44}^k N_{iM} N_{jM} \lhd N_d N_d \rhd_\Omega F_{s,z} F_{\tau,z} + C_{44}^k N_{iP} N_{jM} \lhd N_c N_d \rhd_\Omega F_{s,z} F_{\tau,z} \\
&+ C_{44}^k N_{iM} N_{jP} \lhd N_d N_c \rhd_\Omega F_{s,z} F_{\tau,z} + C_{44}^k N_{iP} N_{jP} \lhd N_c N_c \rhd_\Omega F_{s,z} F_{\tau,z} \\
&+ C_{66}^k \lhd N_{i,x} N_{j,x} \rhd_\Omega F_s F_\tau + C_{26}^k \lhd N_{i,y} N_{j,x} \rhd_\Omega F_s F_\tau + C_{26}^k \\
&\lhd N_{i,x} N_{j,y} \rhd_\Omega F_s F_\tau + C_{22}^k \lhd N_{i,y} N_{j,y} \rhd_\Omega F_s F_\tau
\end{aligned}$$

$$\begin{aligned}
K_{zy}^{k\tau sij} &= C_{44}^k N_{i,yM} N_{jM} \lhd N_d N_d \rhd_\Omega F_{s,z} F_\tau + C_{44}^k N_{i,yM} N_{jP} \lhd N_d N_c \rhd_\Omega F_{s,z} F_\tau \\
&+ C_{45}^k N_{i,xN} N_{jM} \lhd N_a N_d \rhd_\Omega F_{s,z} F_\tau + C_{45}^k N_{i,xN} N_{jP} \lhd N_a N_c \rhd_\Omega F_{s,z} F_\tau \\
&+ C_{44}^k N_{i,yP} N_{jM} \lhd N_c N_d \rhd_\Omega F_{s,z} F_\tau + C_{44}^k N_{i,yP} N_{jP} \lhd N_c N_c \rhd_\Omega F_{s,z} F_\tau \\
&+ C_{45}^k N_{i,xQ} N_{jM} \lhd N_b N_d \rhd_\Omega F_{s,z} F_\tau + C_{45}^k N_{i,xQ} N_{jP} \lhd N_b N_c \rhd_\Omega F_{s,z} F_\tau \\
&+ C_{36}^k \lhd N_i N_{j,x} \rhd_\Omega F_s F_{\tau,z} + C_{23}^k \lhd N_i N_{j,y} \rhd_\Omega F_s F_{\tau,z}
\end{aligned}$$

$$\begin{aligned}
K_{xz}^{k\tau sij} &= C_{45}^k N_{iN} N_{j,yM} \lhd N_a N_d \rhd_\Omega F_s F_{\tau,z} + C_{45}^k N_{iQ} N_{j,yM} \lhd N_b N_d \rhd_\Omega F_s F_{\tau,z} \\
&+ C_{55}^k N_{iN} N_{j,xN} \lhd N_a N_a \rhd_\Omega F_s F_{\tau,z} + C_{55}^k N_{iQ} N_{j,xN} \lhd N_b N_a \rhd_\Omega F_s F_{\tau,z} \\
&+ C_{45}^k N_{iN} N_{j,yP} \lhd N_a N_c \rhd_\Omega F_s F_{\tau,z} + C_{45}^k N_{iQ} N_{j,yP} \lhd N_b N_c \rhd_\Omega F_s F_{\tau,z} \\
&+ C_{55}^k N_{iN} N_{j,xQ} \lhd N_a N_b \rhd_\Omega F_s F_{\tau,z} + C_{55}^k N_{iQ} N_{j,xQ} \lhd N_b N_b \rhd_\Omega F_s F_{\tau,z} \\
&+ C_{13}^k \lhd N_{i,x} N_j \rhd_\Omega F_{s,z} F_\tau + C_{36}^k \lhd N_{i,y} N_j \rhd_\Omega F_{s,z} F_\tau
\end{aligned}$$

$$\begin{aligned}
K_{yz}^{k\tau sij} &= C_{44}^k N_{iM} N_{j,yM} \lhd N_d N_d \rhd_\Omega F_s F_{\tau,z} + C_{44}^k N_{iP} N_{j,yM} \\
&\lhd N_c N_d \rhd_\Omega F_s F_{\tau,z} + C_{45}^k N_{iM} N_{j,xN} \lhd N_d N_a \rhd_\Omega F_s F_{\tau,z} \\
&+ C_{45}^k N_{iP} N_{j,xN} \lhd N_c N_a \rhd_\Omega F_s F_{\tau,z} + C_{44}^k N_{iM} N_{j,yP} \\
&\lhd N_d N_c \rhd_\Omega F_s F_{\tau,z} + C_{44}^k N_{iP} N_{j,yP} \lhd N_c N_c \rhd_\Omega F_s F_{\tau,z} \\
&+ C_{45}^k N_{iM} N_{j,xQ} \lhd N_d N_b \rhd_\Omega F_s F_{\tau,z} + C_{45}^k N_{iP} N_{j,xQ} \\
&\lhd N_c N_b \rhd_\Omega F_s F_{\tau,z} + C_{36}^k \lhd N_{i,x} N_j \rhd_\Omega F_{s,z} F_\tau + C_{23}^k \\
&\lhd N_{i,y} N_j \rhd_\Omega F_{s,z} F_\tau
\end{aligned} \tag{36}$$

$$\begin{aligned}
K_{zz}^{k\tau sij} &= C_{44}^k N_{i,yM} N_{j,yM} \lhd N_d N_d \rhd_\Omega F_s F_\tau + C_{45}^k N_{i,xN} N_{j,yM} \lhd N_a N_d \rhd_\Omega F_s F_\tau \\
&+ C_{44}^k N_{i,yP} N_{j,yM} \lhd N_c N_d \rhd_\Omega F_s F_\tau + C_{45}^k N_{i,xQ} N_{j,yM} \lhd N_b N_d \rhd_\Omega F_s F_\tau \\
&+ C_{45}^k N_{i,yM} N_{j,xN} \lhd N_d N_a \rhd_\Omega F_s F_\tau + C_{55}^k N_{i,xN} N_{j,xN} \lhd N_a N_a \rhd_\Omega F_s F_\tau \\
&+ C_{45}^k N_{i,yP} N_{j,xN} \lhd N_c N_a \rhd_\Omega F_s F_\tau + C_{55}^k N_{i,xQ} N_{j,xN} \lhd N_b N_a \rhd_\Omega F_s F_\tau \\
&+ C_{44}^k N_{i,yM} N_{j,yP} \lhd N_d N_c \rhd_\Omega F_s F_\tau + C_{45}^k N_{i,xN} N_{j,yP} \lhd N_a N_c \rhd_\Omega F_s F_\tau \\
&+ C_{44}^k N_{i,yP} N_{j,yP} \lhd N_c N_c \rhd_\Omega F_s F_\tau + C_{45}^k N_{i,xQ} N_{j,yP} \lhd N_b N_c \rhd_\Omega F_s F_\tau \\
&+ C_{45}^k N_{i,yM} N_{j,xQ} \lhd N_d N_b \rhd_\Omega F_s F_\tau + C_{55}^k N_{i,xN} N_{j,xQ} \lhd N_a N_b \rhd_\Omega F_s F_\tau \\
&+ C_{45}^k N_{i,yP} N_{j,xQ} \lhd N_c N_b \rhd_\Omega F_s F_\tau + C_{55}^k N_{i,xQ} N_{j,xQ} \lhd N_b N_b \rhd_\Omega F_s F_\tau \\
&+ C_{33}^k \lhd N_i N_j \rhd_\Omega F_{s,z} F_{\tau,z}
\end{aligned}$$

References

[1] Zienkiewicz OC, Taylor RL, editors. The finite element method for solid and structural mechanics. Linacre House, Jordan Hill, Oxford: Butterworth-Heinemann; 2005.
[2] Bathe KJ, editor. Finite element procedures. Upper Saddle River, New Jersey: Prentice Hall; 1996.
[3] Hughes TJR, editor. The finite element method. Mineola. New York: Dover Publications; 1987.
[4] Bathe KJ, Dvorkin EN. A four node plate bending element based on Mindlin–Reissner plate theory and mixed interpolation. Int J Numer Methods Eng 1985;21:367–83.
[5] McNeal RH. Derivation of element stiffness matrices by assumed strain distribution. Nucl Eng Des 1982;70:3–12.
[6] Huang HC, Hinton E. A new nine node degenerated shell element with enhanced membrane and shear interpolation. Int J Numer Methods Eng 1986;22:73–92.
[7] Jang J, Pinsky P. An assumed covariant strain based 9-node shell element. Int J Numer Methods Eng 1987;24:2389–411.
[8] Carrera E, Parisch H. An evaluation of geometrical nonlinear effects of thin and moderately thick multilayered composite shells. Compos Struct 1997;40(1):11–24.

[9] Babuska I, Narasimhan R. The Babuska–Brezzi condition and the patch test: an example. Comput Methods Appl Mech Eng 1997;140(17):183–99.
[10] Brezzi F, Bathe K-J, Fortin M. Mixed interpolated elements for Reissner–Mindlin plates. Int J Numer Methods Eng 1990;28:1787–801.
[11] Della Croce L, Scapolla T. Combining hierarchic high order and mixed-interpolated finite elements for Reissner–Mindlin plate problems. Comput Methods Appl Mech Eng 1994;116:185–92.
[12] Della Croce L, Scapolla T. Hierarchic and mixed-interpolated finite elements for Reissner–Mindlin problems. Commun Numer Methods Eng 1995;11:549–62.
[13] Carrera E. Evaluation of layer-wise mixed theories for laminated plates analysis. AIAA J 1998;26:830–9.
[14] Carrera E. Developments, ideas and evaluations based upon the Reissner's mixed variational theorem in the modeling of multilayered plates and shells. Appl Mech Rev 2001;54:301–29.
[15] Carrera E. Historical review of zig-zag theories for multilayered plates and shells. Appl Mech Rev 2003;56:287–308.
[16] Carrera E. Theories and finite elements for multilayered plates and shells: a unified compact formulation with numerical assessment and benchmarking. Arch Comput Methods Eng 2003;10:215–97.
[17] Carrera E, Demasi L. Multilayered finite plate element based on Reissner mixed variational theorem. Part II: numerical analysis. Int J Numer Methods Eng 2002;55:253–96.
[18] Carrera E, Boscolo M. Classical and Mixed elements for static and dynamic analysis of piezoelectric plates. Int J Numer Methods Eng 2007;70:253–91.
[19] Carrera E, Nali P. Mixed piezoelectric plate elements with direct evaluation of transverse electric displacement. Int J Numer Methods Eng 2009;80:403–24.
[20] Reissner E. The effect of transverse shear deformation on the bending of elastic plates. J Appl Mech 1945;12:69–76.
[21] Mindlin RD. Influence of rotatory inertia and shear in flexural motions of isotropic elastic plates. J Appl Mech 1951;18:28–31.
[22] Kirchhoff G. Uber das Gleichgewicht und die Bewegung einer elastishen Scheibe. Crelles J 1850;40:51–88.